

Supporting Information for:

Nanoparticles self-assembled from multiple interactions: a novel near-infrared fluorescent sensor for detection of serum albumin in human sera and turn-on live-cell imaging

Xiaopeng Fan[‡], Qingyuan He[‡], Shiguo Sun, Hongjuan Li, Yuxin Pei and Yongqian

Xu*

College of Science, Northwest A&F University, Yangling, Shaanxi, P.R. China, 712100, xuyq@nwsuaf.edu.cn

1. Experimental

1.1 Synthesis material and instruments

All chemicals and reagents were used directly as obtained commercially unless otherwise noted. Water used was ultra filter deionized. Avidin, concanavalin, myoglobin, casein, lysozyme, RNaseA, trypase, pepsin, thrombin, BSA, casein were purchased from SIGMA. NMR spectra were recorded on a Varian 300 Gemini spectrometer. Mass spectrum was obtained in ESI mode on a HP1100LC/MSD mass spectrometer. UV-Vis spectra were acquired on a Shimadzu 1750 UV-visible spectrometer. Fluorescence spectra were obtained on a RF-5301 fluorescence spectrometer.

1.2 Measurement Procedures

The stock solutions of **SQ-P** with a concentration of 5.0×10^{-4} M were prepared first by dissolving the appropriate amount of the dye in DMSO, respectively. For measurement of spectroscopic properties, 30 μ L of each stock solution were diluted with PBS (0.01 M, 3 mL, pH 7.2) to obtain aqueous solution of **SQ-P** (5.0×10^{-6} M) under vigorous stirring at room temperature. Stock solutions of the various proteins

were prepared in deionized water and the concentrations were fixed at 6×10^{-4} M. The quantum yield of fluorescence of the sample was measured using bis(3-ethylbenzothiazol-2-ylidene)squaraine in ethanol ($\Phi = 0.21$) as a standard^{s1} and calculated using eq 1:

$$\Phi_{\text{unk}} = \Phi_{\text{std}} \times \left(\frac{I_{\text{unk}}}{I_{\text{std}}} \right) \times \left(\frac{A_{\text{std}}}{A_{\text{unk}}} \right) \times \left(\frac{n_{\text{unk}}}{n_{\text{std}}} \right)^2 \quad (1)$$

Where Φ_{unk} is the fluorescence quantum yield of the sample, Φ_{std} is the fluorescence quantum yield of the standard, I_{unk} and I_{std} are the integrated emission intensities of the sample and the standard, respectively, A_{unk} and A_{std} are the absorbance of the sample and the standard at the excitation wavelength, respectively, and n_{unk} and n_{std} are the refractive indexes of the corresponding solution.

The preparation of deproteinized human blood samples is followed the reported literature.^{S2} Human blood samples were collected from healthy volunteers treated in the local Medical Hospital. All samples were obtained by venipuncture and collected in heparinized vacutainer tubes. Then, a 200 μL aliquot of the blood was deproteinized by mixing immediately with 400 μL of cold 10% Cl_3CCOOH . After vortex mixing, the mixture was centrifuged at 8000 rpm for 10 min. A total of 400 μL of the supernatant was collected. Then Cl_3CCOOH was evaporated out. The obtained supernatant without Cl_3CCOOH was ready for assays.

1.3 Atomic Force Microscopy (AFM) and Field emission scanning electron microscope (FESEM)

Samples for the imaging were prepared by spin-casting the **SQ-P** in the absence and presence of its specific protein (BSA) at the specified concentrations. AFM (Nanoscope V) was performed in the ambient air condition in the tapping mode, a frequency near resonance. The scan rate was 1 Hz with a scan field of view of 500 nm \times 500 nm to 5 μm \times 5 μm . The microstructure of the samples was analyzed by field emission scanning electron microscopy (FESEM, S-4800). All samples were dried and detected at room temperature with SE detection at 10.0 kV. DLS measurements were performed on a DelsaTM Nano system (Beckman Coulter, Inc., CA, U.S.A.).

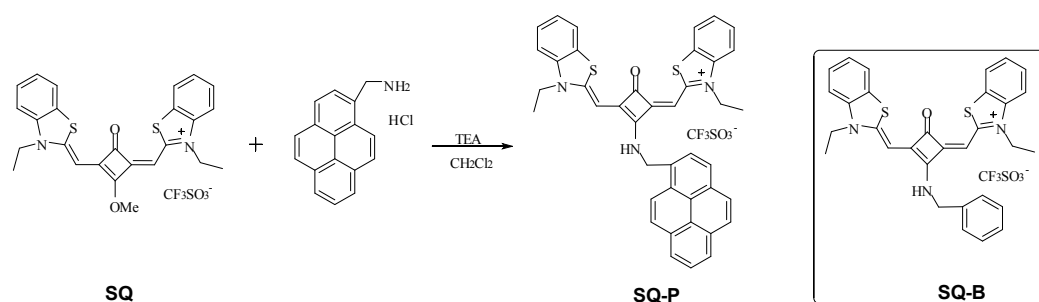
1.4 Cell culture and fluorescence image

HeLa cells were seeded on 35 mm glass-bottomed dishes (NEST) and incubated in RPMI-1640 in an incubator (37 °C, 5% CO₂ and 20% O₂) for 24 h. The cells were rinsed slightly 3 times with fresh RPMI-1640 and incubated in RPMI-1640 medium spiked with or without sensor (5 μM) for 30 min, respectively. After washing with fresh RPMI-1640, the cells treated with sensor were further incubated in fresh RPMI-1640 containing of 50 μM hydrazine for 0.5 h. Cells were then analyzed by Laser Scanning Confocal Microscope (A1R).

1.5 Calculation of detecting limit

Detecting limit $DL = K \times S_{b1} / S$, where $K=3$, S_{b1} is the standard derivation of the blank solution and S is the slope of the calibration curve.^{S3}

1.6 Synthesis of **SQ-P** and **SQ-B**

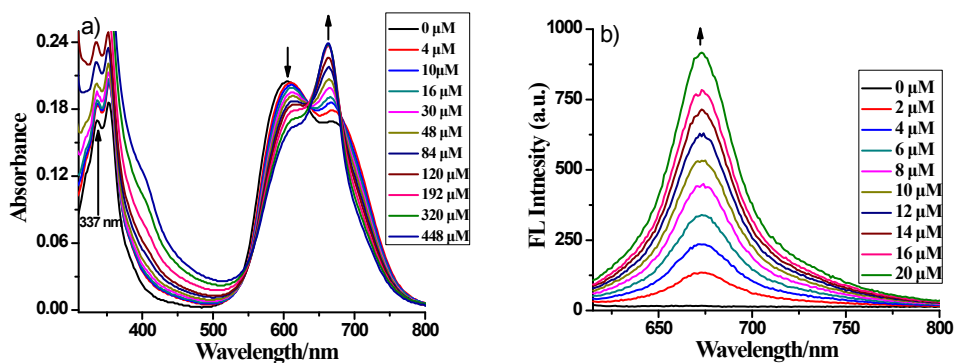


The compound **SQ** was synthesized according to the procedure reported previously.^{S4}

SQ-P was synthesized by using a modified procedure (Santos et al, 2005). 1-aminomethylpyrene hydrochloride (0.38 mmol, 102 mg) and triethylamine (0.76 mmol, 106 μL) were dissolved in 130 mL anhydrous CH₂Cl₂. The solution was refluxed under nitrogen atmosphere for 2 h and cooled to room temperature. **SQ** (0.338 mmol, 200 mg) was added to above solution under nitrogen atmosphere, and the resulting solution was further at room temperature for 48 h. The solvent was removed under reduced pressure and the residue was applied to silica gel chromatograph (by using as CH₂Cl₂/MeOH eluent) to get solid **SQ-P** (250 mg, 93 %). ¹H NMR (500 MHz, DMSO-*d*₆) δ 9.44 (t, $J = 5.6$ Hz, 1H), 8.49 (d, $J = 9.3$ Hz, 1H), 8.43-8.31 (m, 4H), 8.27-8.17 (m, 2H), 8.18-8.09 (m, 2H), 8.01 (d, $J = 7.9$ Hz, 1H),

7.84 (d, $J = 7.8$ Hz, 1H), 7.70 (d, $J = 8.4$ Hz, 1H), 7.54 (t, $J = 7.7$ Hz, 1H), 7.41 (s, 1H), 7.33 (d, $J = 2.8$ Hz, 2H), 7.24 (m, , 1H), 6.35 (s, 1H), 5.67 (d, $J = 5.5$ Hz, 2H), 5.51 (s, 1H), 4.30 (d, $J = 7.1$ Hz, 2H), 3.58 (d, $J = 7.0$ Hz, 2H), 1.34 (t, $J = 7.1$ Hz, 3H), 0.25 (t, $J = 7.1$ Hz, 3H). ^{13}C NMR (126 MHz, $\text{DMSO-}d_6$) δ 173.89, 163.88, 161.12, 158.93, 157.21, 155.92, 140.21 ,139.97, 131.26, 130.81, 130.51, 130.26, 128.24, 127.94, 127.84, 127.51, 127.33, 126.55, 125.71, 125.50, 125.23, 125.13, 125.08, 124.40, 124.19, 123.81, 123.03, 122.53, 122.48, 113.30, 112.64, 86.53, 86.41, 45.26, 41.70, 40.38, 12.60, 11.23. MS (ESI+) found 646.23 (M)⁺, calcd for $\text{C}_{41}\text{H}_{32}\text{N}_3\text{OS}_2$, 646.84.

For comparison, a similar compound **SQ-B** was also synthesized, where the pyrene group was replaced by phenyl group. The synthesis of the compound **SQ-B** is similar to that of **SQ-P** by using 1-aminomethylphenyl hydrochloride to replace 1-aminomethylpyrene hydrochloride. ^1H NMR (500 MHz, $\text{DMSO-}d_6$, ppm) δ 9.29 (t, $J = 6.1$ Hz, 1H), 8.00 (d, $J = 7.8$ Hz, 1H), 7.90 (d, $J = 7.8$ Hz, 1H), 7.72 (d, $J = 8.3$ Hz, 1H), 7.56 (dd, $J = 17.7, 8.3$ Hz, 2H), 7.51-7.43 (m, 5H), 7.43 – 7.28 (m, 3H), 6.32 (s, 1H), 5.72 (s, 1H), 4.92 (d, $J = 6.1$ Hz, 2H), 4.39-4.30 (m, 2H), 4.18 (q, $J = 6.8$ Hz, 2H), 1.36 (t, $J = 7.2$ Hz, 3H), 1.08 (t, $J = 6.3$ Hz, 3H). ^{13}C NMR (126 MHz, $\text{DMSO-}d_6$) δ 173.84, 163.73, 161.07, 159.33, 157.17, 156.76, 140.28 , 129.01, 128.00 , 127.81, 127.74, 127.66, 126.89, 125.12, 124.58, 123.06, 122.69, 113.33, 112.87, 86.60, 86.30, 46.86, 41.75, 40.97, 12.60, 12.19.



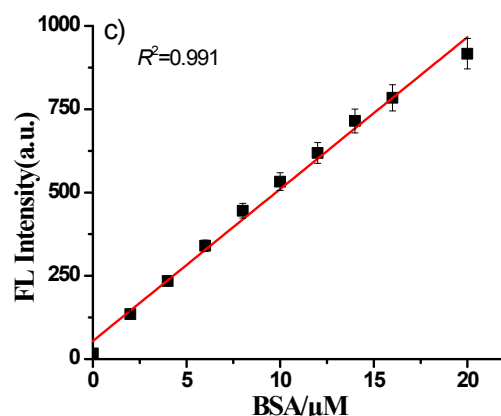


Fig. S1 Spectroscopic response of **SQ-P** to BSA. (a) UV-Vis absorption change of **SQ-P** (5 μM) upon addition of BSA (0-448 μM). (b) Fluorescence spectral changes of **SQ-P** (5 μM) upon addition of BSA (0-20 μM) (λ_{ex} = 600 nm, slit width of excitation and emission is 10 and 10 nm, respectively). Fluorescence measurements were performed 1 min after adding BSA to the **SQ-P** solution. (c) Plot of the fluorescence intensity at 668 nm to BSA concentrations (0-20 μM). All experiments were performed in 10 mM PBS buffer (pH 7.2).

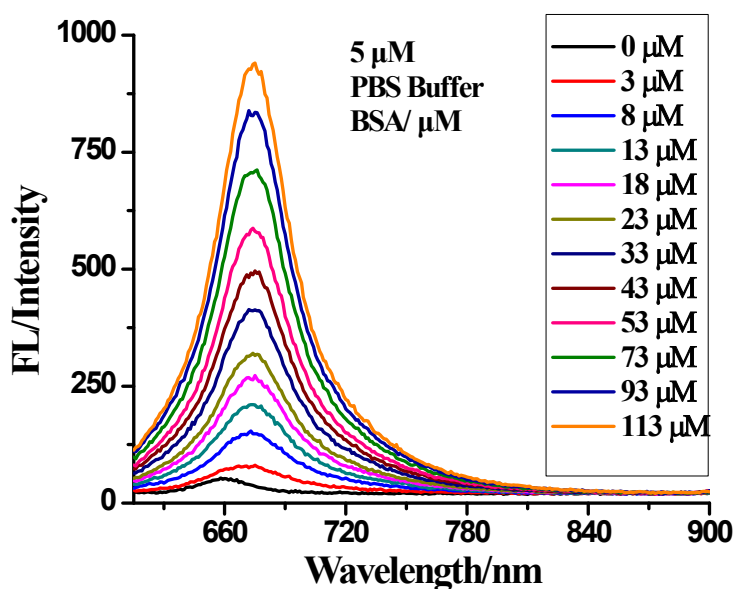


Fig. S2. Fluorescence spectral changes of **SQ-B** (5 μM) upon addition of BSA (0-113 μM) (λ_{ex} = 600 nm, slit width of excitation and emission is 10 and 5 nm, respectively). Fluorescence measurements were performed 1 min after adding BSA to the **SQ-B** solution.

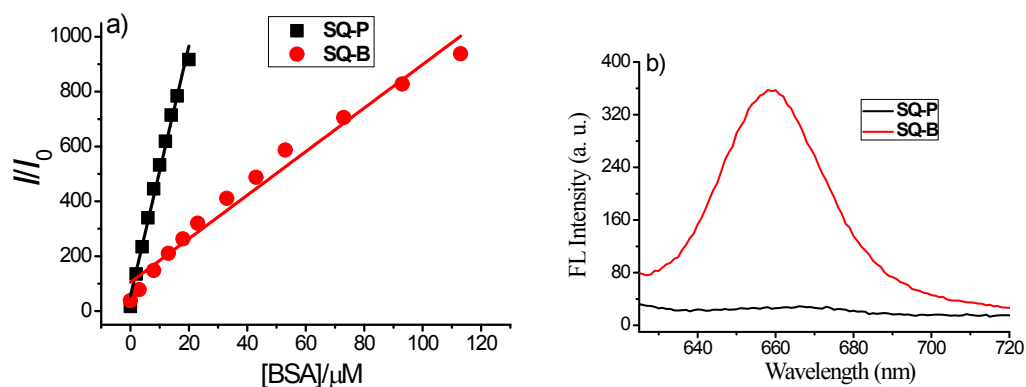


Fig. S3. (a) Plots of the fluorescence intensities of **SQ-P** at 668 nm and **SQ-B** at 674 nm to BSA concentrations. (b) The fluorescence spectra of **SQ-P** and **SQ-B** in the absence of BSA, where $I_{\text{SQ-B}}/I_{\text{SQ-P}}$ at 660 nm is about 13.7-fold. All experiments were performed in 10 mM PBS buffer (pH 7.2), $\lambda_{\text{ex}} = 600$ nm, slit width of excitation and emission is 10 and 10 nm, respectively.

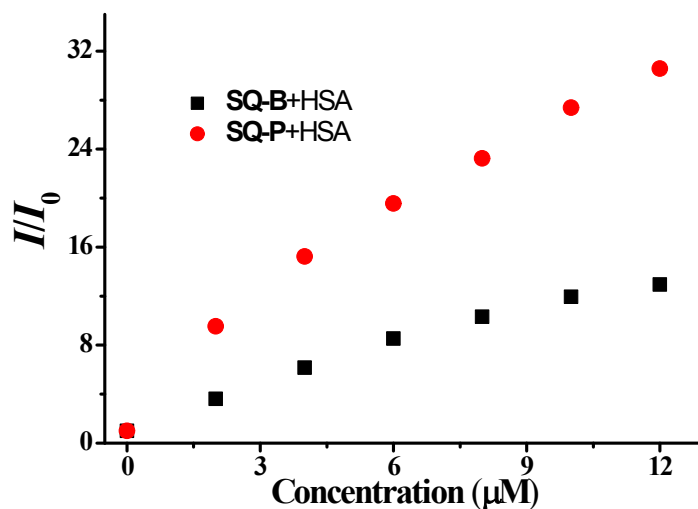


Fig. S4. Plots of the fluorescence intensities of **SQ-P** at 674 nm and **SQ-B** at 674 nm to HSA concentrations. All experiments were performed in 10 mM PBS buffer (pH 7.2).

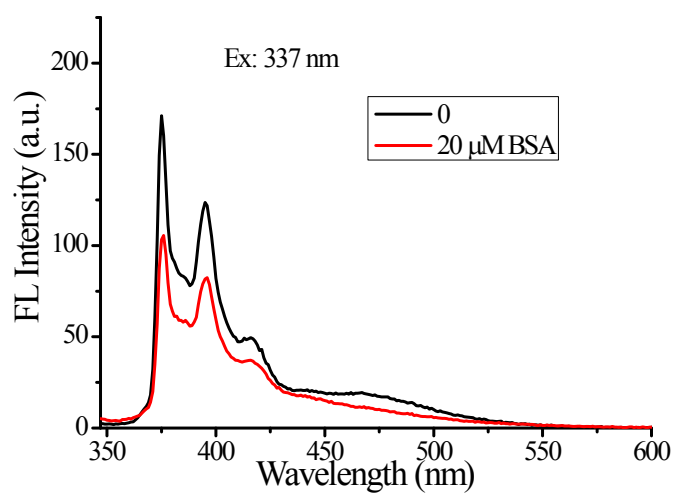


Fig. S5. Fluorescence spectral changes of **SQ-P** (5 μM) upon addition BSA (20 μM) ($\lambda_{\text{ex}} = 337 \text{ nm}$) in PBS buffer (10 mM, pH=7.2).

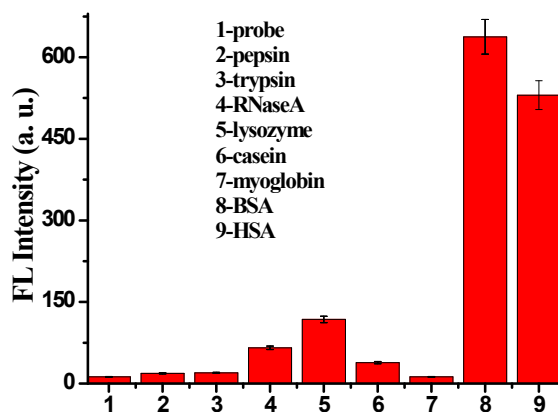


Fig. S6 Selectivity test of **SQ-P** with other non-targeted proteins. **SQ-P** (5 μM) was tested with non-targeted proteins at 20 μM . Bars represent fluorescence intensity at 684 nm.

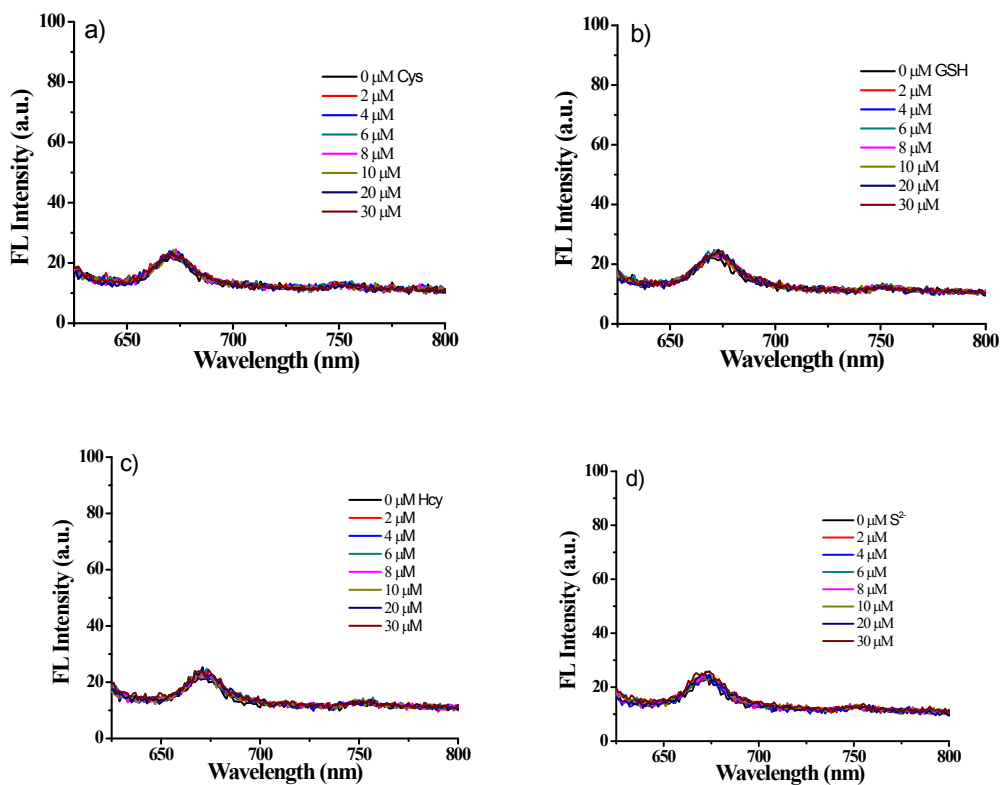


Fig. S7. Fluorescence spectral changes of SQ-P (5 μM) upon addition of thiol-containing compounds (20 μM) ($\lambda_{\text{ex}} = 600 \text{ nm}$) in PBS buffer (10 mM, pH=7.2). a) Cys. b) GSH. c) Hcy. d) S^{2-} .

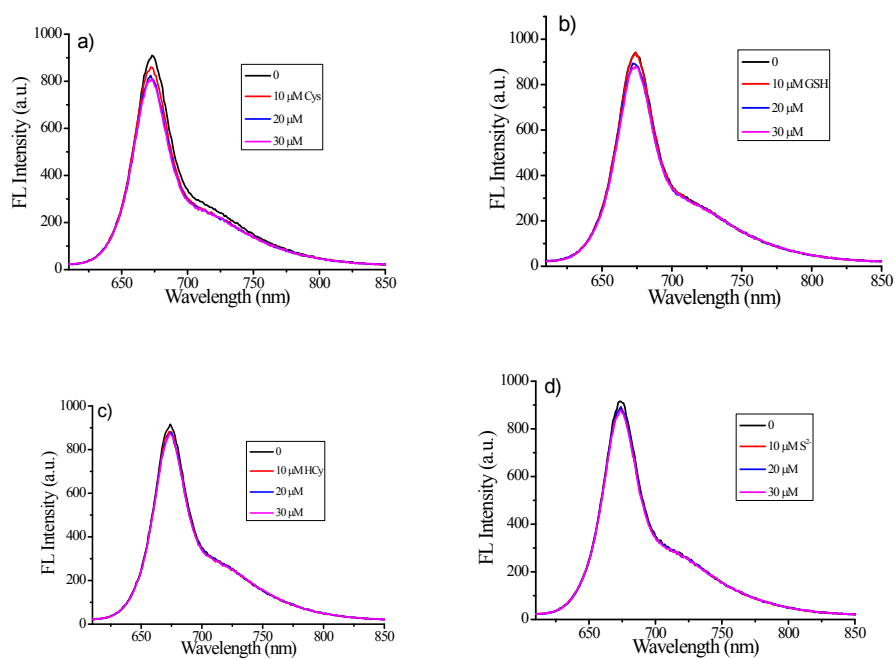


Fig. S8. Fluorescence spectral changes of **SQ-P** (5 μM) upon addition of thiol-containing compounds (20 μM) ($\lambda_{\text{ex}} = 600 \text{ nm}$) in PBS:CH₃CN=1:1 (10 mM, pH=7.2) (10 mM, pH=7.2), where **SQ-P** exists in monomer state. a) Cys. b) GSH. c) Hcy. d) S²⁻.

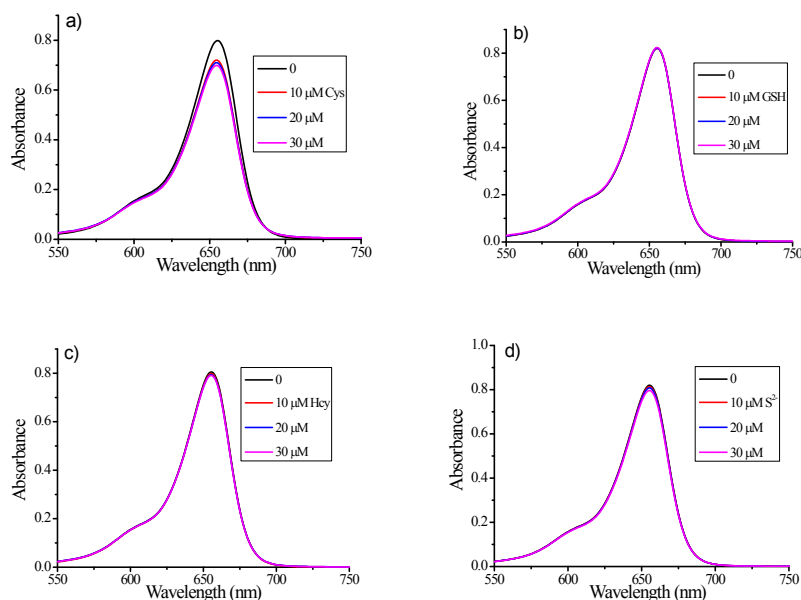
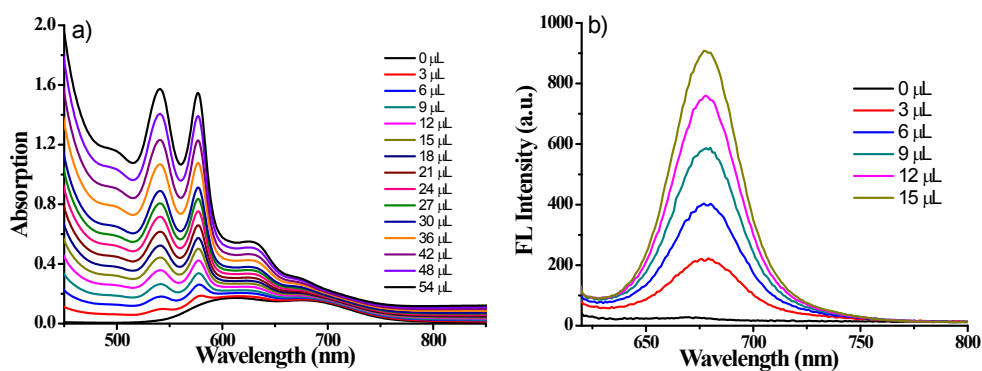


Fig. S9. Absorption changes of **SQ-P** (5 μM) upon addition of thiol-containing compounds (20 μM) ($\lambda_{\text{ex}} = 600 \text{ nm}$) in PBS:CH₃CN=1:1 (10 mM, pH=7.2) (10 mM, pH=7.2), where **SQ-P** exists in monomer state. a) Cys. b) GSH. c) Hcy. d) S²⁻.



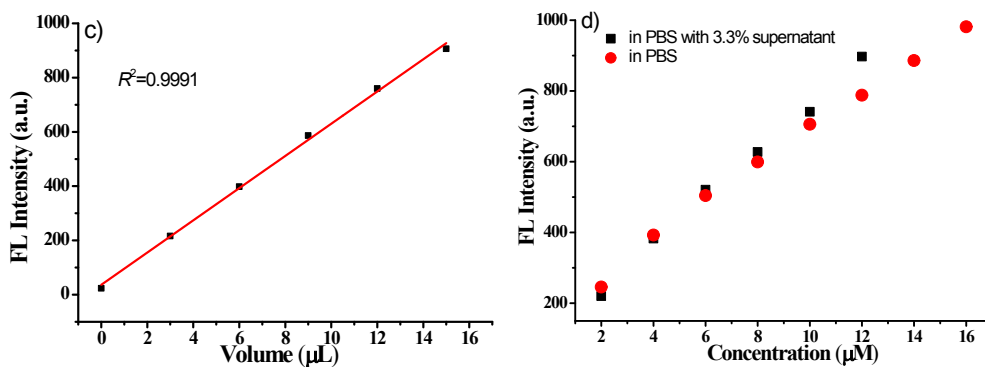


Fig. S10 Spectroscopic response of **SQ-P** to human blood serum. (a) UV-Vis absorption change of **SQ-P** (5 μM) upon addition of blood sample (0-54 μL). (b) Fluorescence spectral changes of **SQ-P** (5 μM) upon addition of blood sample (0-15 μL) ($\lambda_{\text{ex}} = 600 \text{ nm}$). Fluorescence measurements were performed 1 min after adding blood sample to the **SQ-P** solution. (c) Plot of the fluorescence intensity at 668 nm to blood sample volumes (0-15 μL). (d) Plot of the fluorescence intensity at 668 nm to addition of HSA with and without 3.3% deproteinized blood sample. All experiments were performed in 10 mM PBS buffer (pH 7.2).

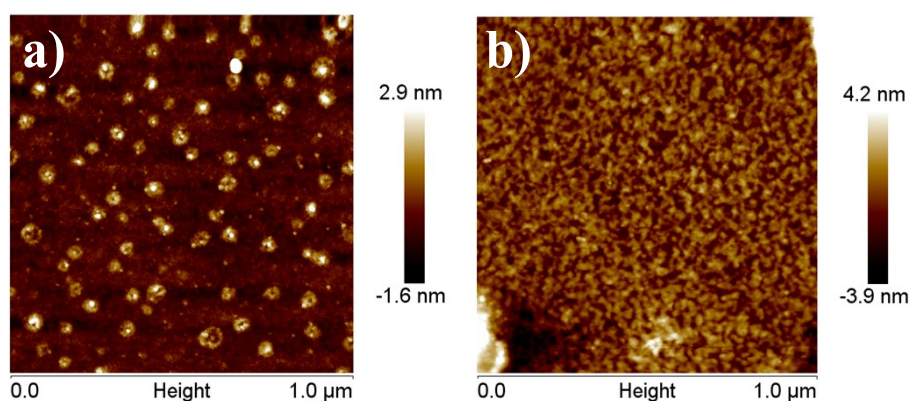


Fig. S11 AFM images of **SQ-P**. a) **SQ-P** alone. b) **SQ-P** and BSA. The solution concentrations used for film preparation are 5 μM for **SQ-P** and 20 μM for BSA in PBS buffer and the scale is 1 μM .

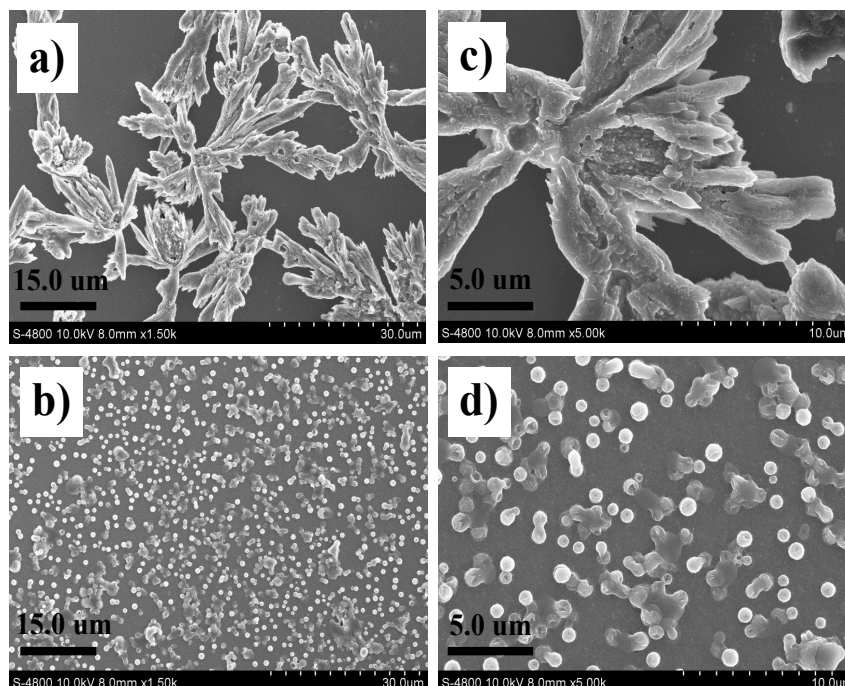


Fig. S12 FESEM images of **SQ-P**. (a) and (c): **SQ-P** alone. (b) and (d): **SQ-P** and BSA. The solution concentrations used for film preparation are 5 μM for **SQ-P** and 20 μM for BSA in PBS buffer.

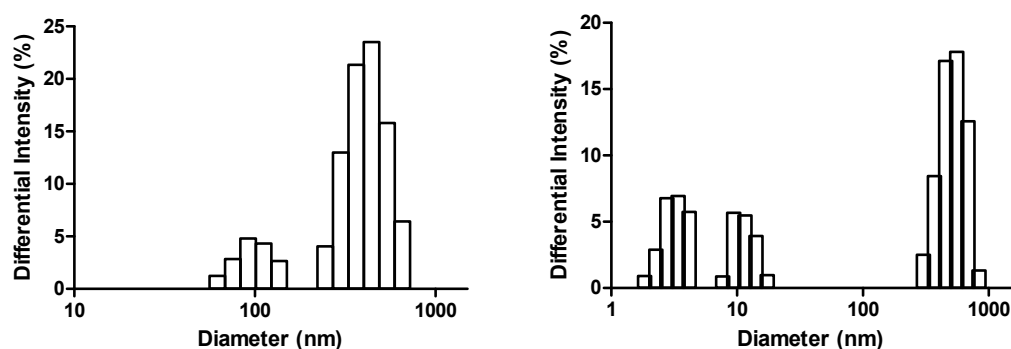


Fig. S13. DLS analysis of **SQ-P** (5 μM) solution (10 mM PBS buffer, pH 7.2) in the absence (left) and presence (right) of 200 μM BSA. DLS data of BSA protein alone (6 μM) is also obtained.

The intensity of large particles (~ 700 nm) assigned to “large” aggregates (oligomer) reduced after adding serum albumin, suggesting that the equilibrium between monomer and aggregates shifts along the direction of monomer.

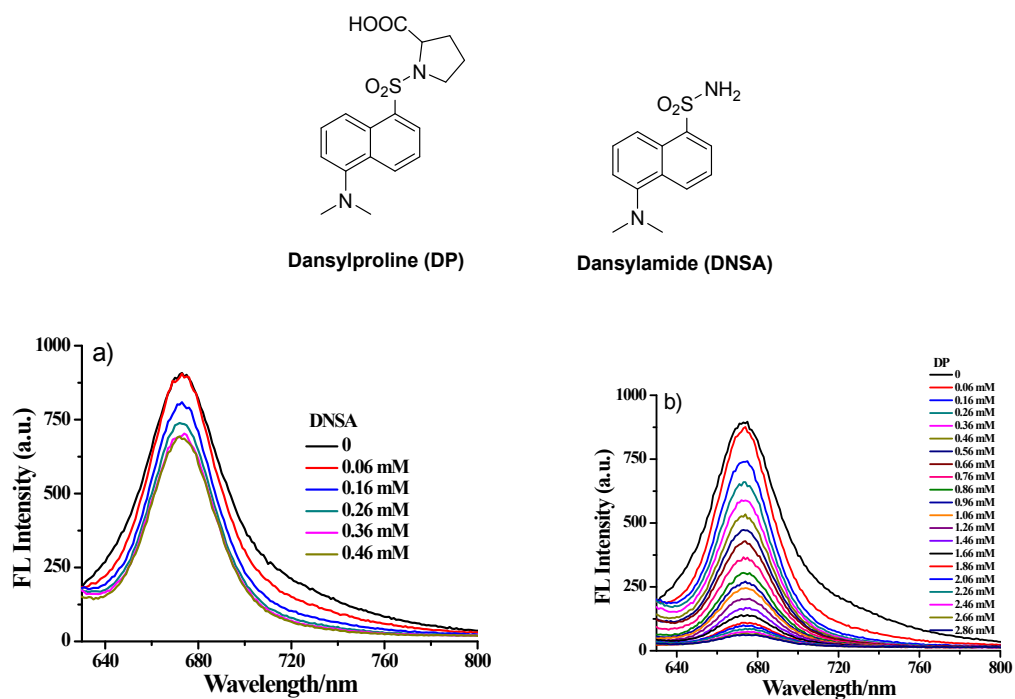


Fig. S14. Fluorescence of SQ-P (5 μ M) in phosphate buffer solution (10 mM, pH7.2) with different concentration of DNSA (a) and DP (b) in the presence of 25 μ M BSA.

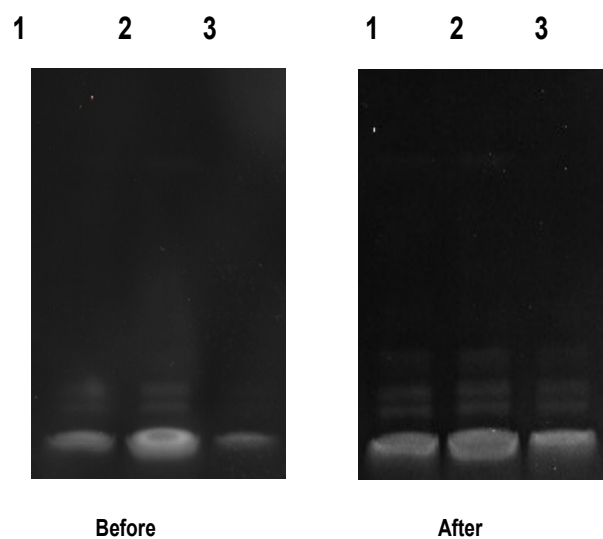


Fig. S15. Fluorescence images of BSA stained by SQ-P after electrophoresis. (1) BSA 10 μ g, (2) 110 μ g, (3) 2 μ g before and after washing.

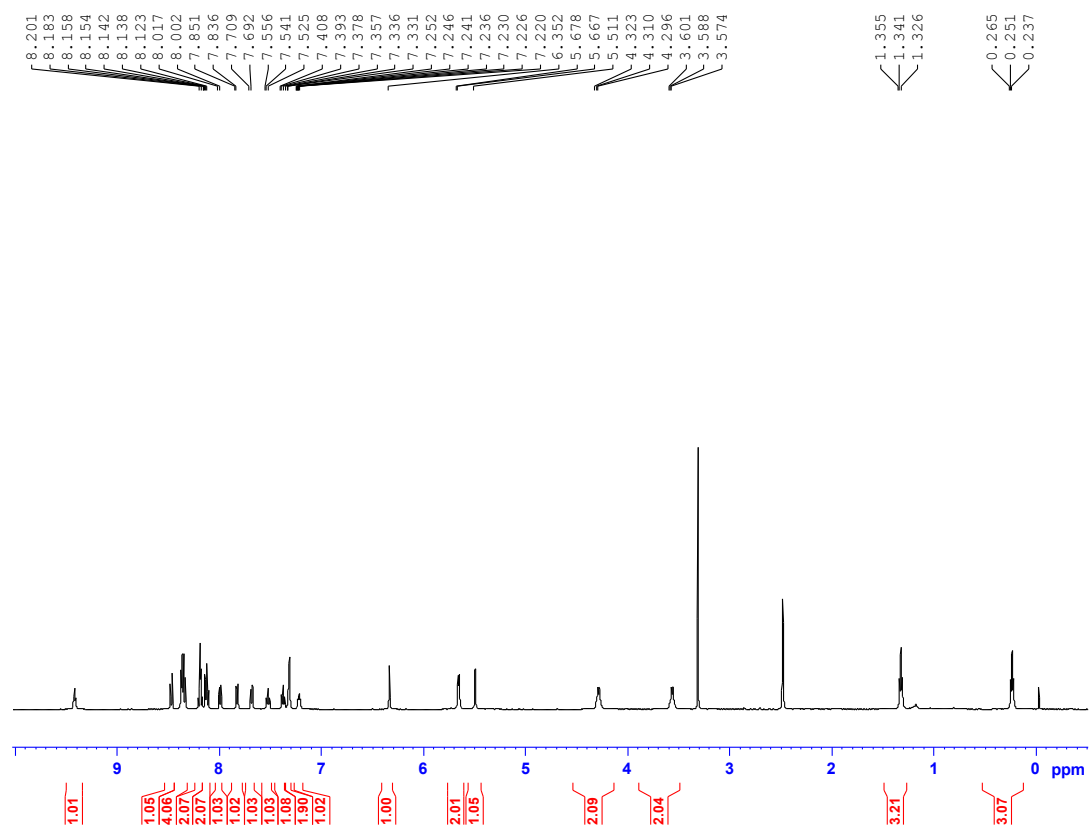


Fig. S16. ^1H NMR of SQ-P in $\text{DMSO-}d_6$ solvent. The signals at 3.3 and 2.5 ppm are attributed to H_2O and DMSO, respectively.

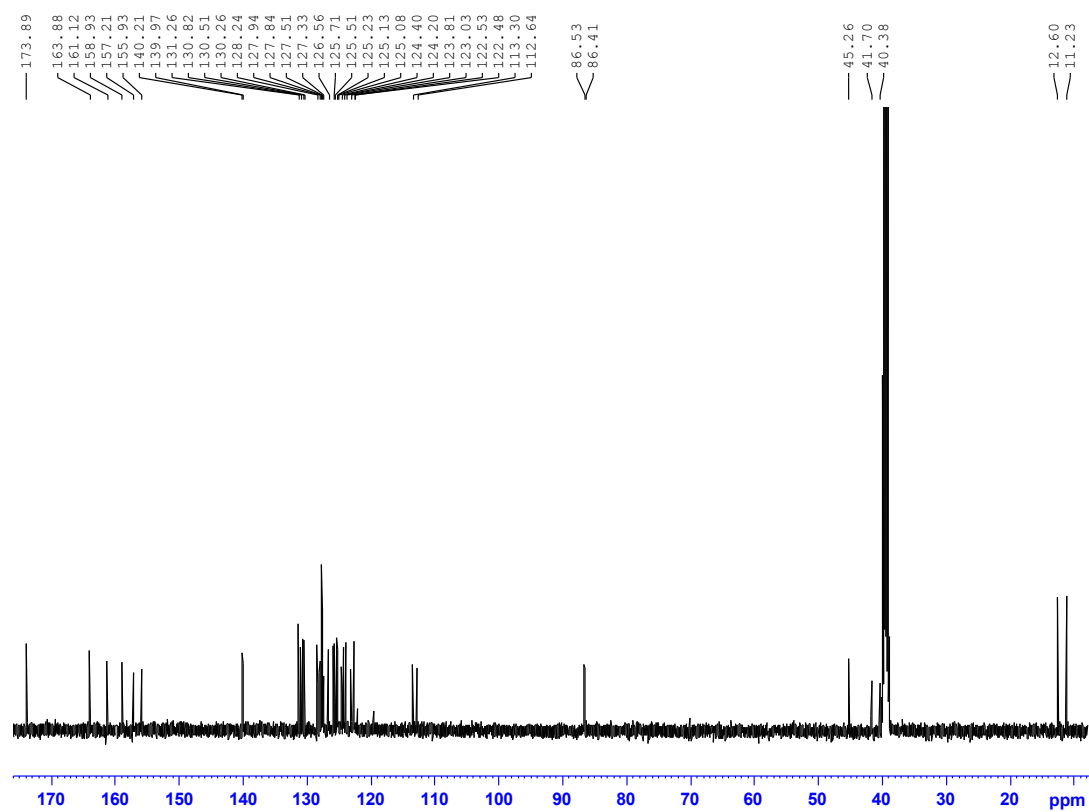


Fig. S17. ^{13}C NMR of SQ-P in $\text{DMSO-}d_6$ solvent. The signal at 39.52 ppm is attributed to DMSO.

[SSG]-H-1 #2-8 RT: 0.00-0.03 AV: 7 NL: 6.56E4
T: ITMS + c ESI sid=35.00 Full ms [50.00-2000.00]

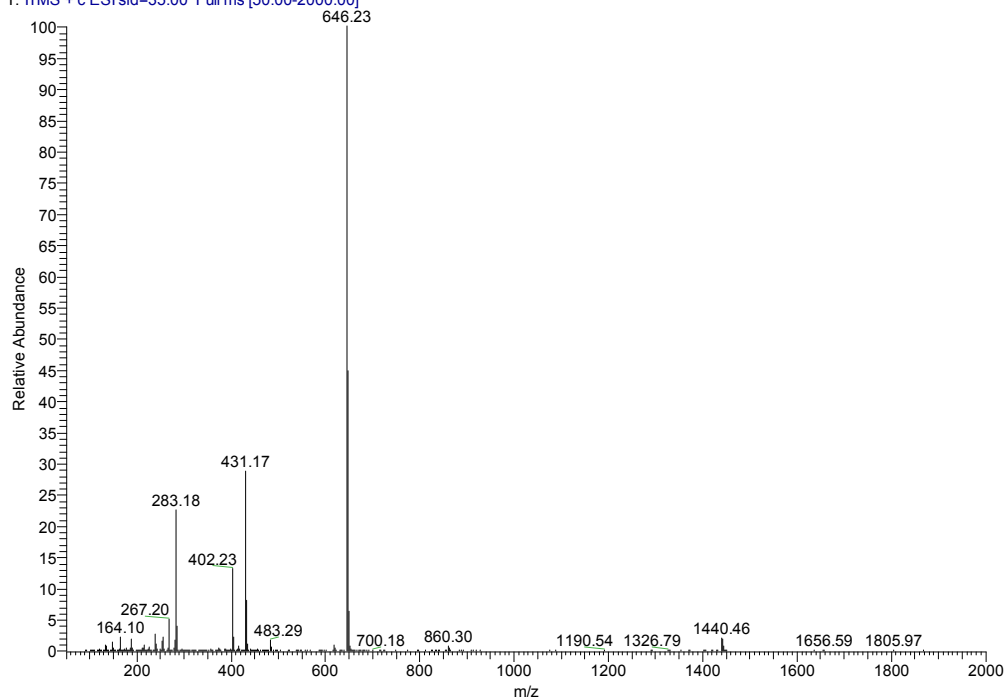


Fig. S18. MS spectrum of SQ-P.

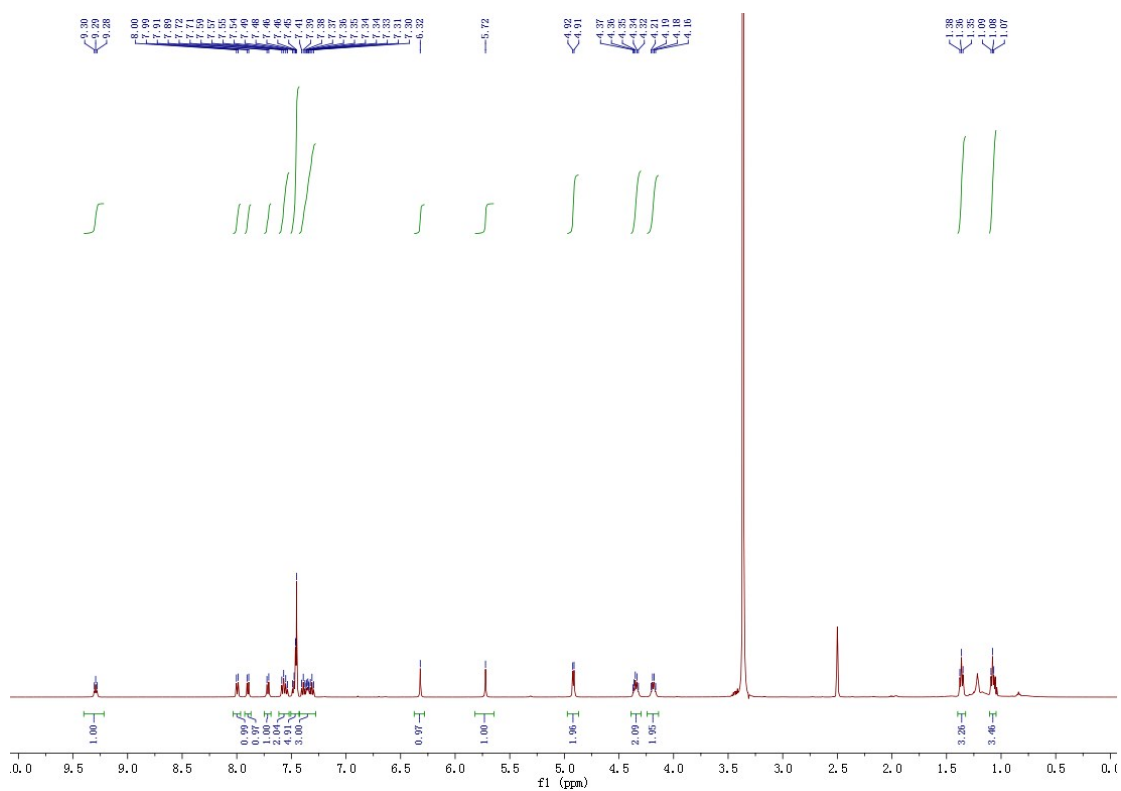


Fig. S19. ^1H NMR of SQ-B in $\text{DMSO}-d_6$ solvent. The signals at 3.3 and 2.5 ppm are attributed to H_2O and DMSO, respectively.

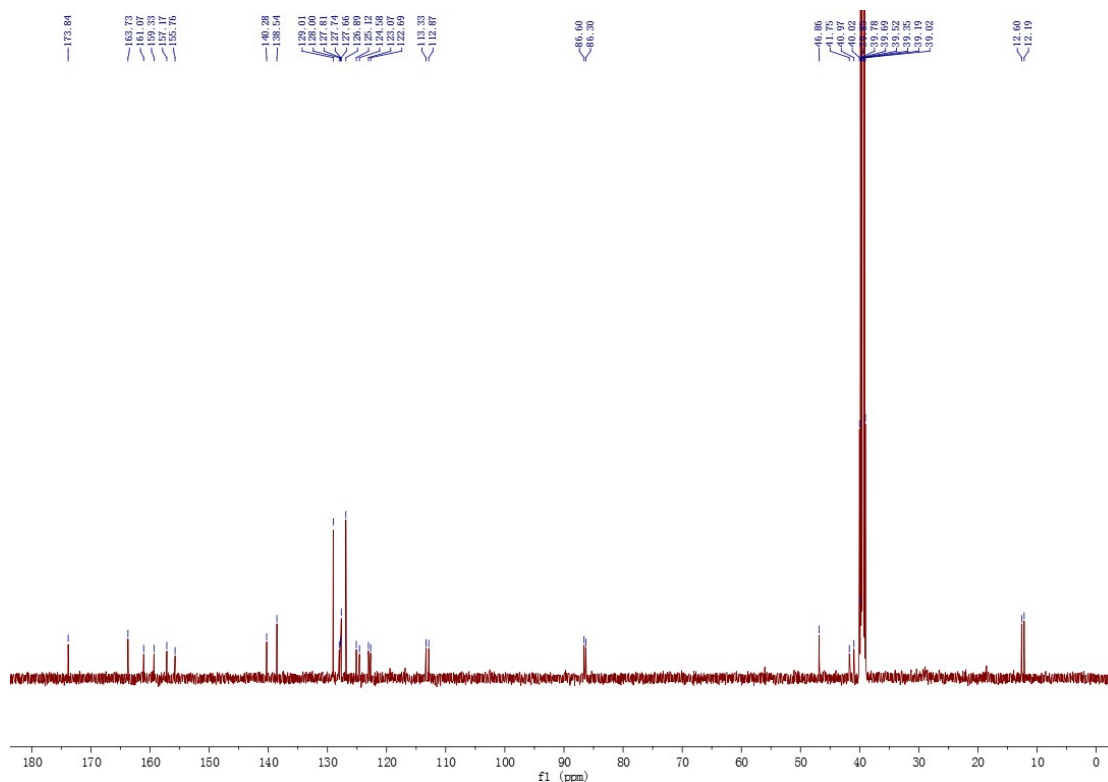


Fig. S20. ^{13}C NMR of **SQ-B** in DMSO- d_6 solvent. The signal at 39.52 ppm is attributed to DMSO.

S1 S. Das, K. G. Thomas, R. Ramanathan, M. V. George and P. V. Kamat, *J. Phys. Chem.* **1993**, *97*, 13625.

S2 D. Tian, Z. Qian, Y. Xia and C. Zhu, *Langmuir*, 2012, *28*, 3945.

S3 A. Hakonen, *Anal. Chem.*, 2009, **81**, 4555.

S4 Y. Xu, Z. Li, A. Malkovskiy, S. Sun and Y. Pang, *J. Phys. Chem. B*, 2010, **114**, 8574.